2. Tiwari, C. M., Agrawal, S. P., Tiwari, D. P., Elbori, M. A. and Shrivastava, P. K., Study of daily variation of cosmic ray intensity for the period of 1989–2000. *Curr. Sci*., 2003, **83**, 219–222.
3. Tiwari, C. M., Tiwari, D. P. and Shrivastava, P. K., Anomalous behavior of cosmic ray diurnal anisotropy during descending phase of the solar cycle-22. *Curr. Sci*., 2005, **88**, 1275–1278.
4. Jerlov, N., Olsson, H. and Schuepp, W., Measurements of solar radiation at Loevanger in Sweden during the total eclipse 1945. *Tellus*, 1954, **6**, 44–45.
5. Koepke, P., Reuder, J. and Schween, J., Spectral variation of the solar radiation during an eclipse. *Meteorol. Z.*, 2001, **10**, 179–186.
6. Sharp, W. E., Silverman, S. M. and Lloyd, J. W. F., Summary of sky brightness measurements during eclipses of the sun. *Appl. Opt*., 1971, **10**, 1207–1210.
7. Zerofos, C. S. *et al.*, Evidence of gravity waves into the atmosphere during the march 2006 total solar eclipse. *Atmos. Chem. Phys. Discuss*., 2007, **7**, 4943–4951.
8. Founda, D. *et al.*, The effect of total solar eclipse of 29 March 2006 on meteorological variables in Greece. *Atmos. Chem. Phys. Discuss*., 2007, **7**, 10631–10667.
9. Chintalapudi, S. N. *et al.*, γ ray and X-ray measurements during total solar eclipse on 24 October 1995 at Diamond Harbour. *Kodaikanal Obs. Bull*., 1997, **13**, 225–234.
10. Bhattacharya, A. *et al.*, Variation of γ-ray and particle fluxes at the sea level during the total solar eclipse of 24 October 1995. *Astrophys. Space Sci*., 1997, **250**, 313–326.
11. Antonova, V. P., Volodichev, N. N., Kryukov, S. V., Chubenko, A. P. and Shchepetov, A. L., Effect of solar eclipses on neutron flux variations at the earth's surface. *Bull. Rus. Acad. Sci. Phys.*, 2007, **71**, 1054–1057.
12. Bhattacharya, A. B. and Bhattacharya, R., Recovery effect in the field intensity of atmospherics. *Indian J. Radio Space Phys*., 1983, **12**, 30–32.
13. Bhattacharya, A. B., Dutta, B. K. and Bhattacharya, R., A comparative study of the sunrise and sunset effects on the integrated field intensity of VLF atmospherics. *Ann. Geophys*., 1995, **13**, 976–980.
14. Dutta, G., Joshi, M. N., Pandarinath, N., Bapiraju, B., Srinivasan, S., Subha Rao, J. V. and Aleem, B. H., Wind and temperature over Hyderabad during the solar eclipse of 24 October 1995. *Indian J. Radio Space Phys*., 1999, **28**, 11–14.
15. Bhattacharya, A. B., Kar, S. K., Bhattacharya, R. and Sen, A. K., Response of the atmosphere to the solar activity variations. In Proceedings of the Frontiers of Radio Science, INCURSI-96, Calcutta, 1996, pp. 16–20.
16. Solar geophysical data explanation, NOAA, 1980, **426**.
17. Svensmark, H., Influence of cosmic rays on earth's climate. *Phys. Rev. Lett*., 1998, **81**, 5027–5030.
18. Bhattacharya, A. B., Kar, S. K., Bhattacharya, R. and Basak, J., Measurements of field intensity of radio signals, atmospheric noise and UV radiation during the total solar eclipse of 24 October 1995. *Indian J. Radio Space Phys*., 1996, **25**, 173–174.
19. Kandemir, G., Guclü, M. C., Geckinli, M., Firat, C., Boydag, S., Özgüc, A. and Yasar, T., Variation of cosmic ray intensity during the solar eclipse 11 August 1999, ASP Conference Series, 2000, **205**, 202–207.
20. Aculinin, A. and Smicov, V., Ground based observation of short wave solar radiation during solar eclipse on October 3, 2005 in Chisinau, Moldova. *Mal. J. Phys. Sci*., 2006, **5**, 117–120.
21. Kazadzis, S. *et al.*, Effects of total solar eclipse of 29 March 2006 on surface radiation. *Atmos. Chem. Phys.*, 2007, **7**, 9235–9258.

ACKNOWLEDGEMENTS. We thank the India Meteorological Department and NOAA, USA for the required data. Financial support from UGC, New Delhi is acknowledged. We also thank the anonymous referees for their valuable comments.

Received 12 October 2009; revised accepted 12 May 2010

Anomalous cooling over the Arabian Sea during February 2008

Anant Parekh

Theoretical Studies Division, Indian Institute of Tropical Meteorology, Pune 411 008, India

Satellite observations over the Arabian Sea revealed anomalous cooling in February 2008 associated with the anomalous north westerly winds from the continent. Land–sea air temperature contrast (relative humidity difference) between Arabia and Arabian Sea is 6–8°C (40%) during the cooling event. This condition supports a loss of heat flux (180–200 W/m^2) from ocean to atmosphere via evaporation. Enhancement of biological activity associated with the cooling is also confirmed. Deepening of the mixed layer via convective and wind forced mixing is observed. Advective heat flux analysis deduces that heat gain via Ekman flow is slightly higher at southern boundary but geostrophic meridional overturning (diffusion of heat flux) is close to the climatic mean. Heat gains via Ekman flow oppose cooling. Thus resultant cooling is mainly due to loss of heat flux (65–95 W/m^2) to the atmosphere; major contributor is latent heat flux.

Keywords: Arabian Sea, Ekman flow, heat flux, sea surface temperature.

THE Arabian Sea (AS) temperature follows bimodal annual cycle[1,2]. It has cooling phases during January–February and July–August, first one is during winter monsoon (low winds and dry atmosphere) and second one is during summer monsoon (high winds and humid atmosphere). Warming phase occurs during April–May and October–November[3]. This rise and fall of sea surface temperature (SST) plays an important role in air–sea interaction[4,5], monsoon evolution[6] and biological activity of the basin[7–9]. It is also reported that SST plays a crucial role as a boundary parameter for atmospheric general circulation models[10]. SST over the Indian Ocean during December–February has significant positive correlation with Indian summer monsoon rainfall on the tropical biennial oscillation time scale[11] rather than Pacific SST.

The present study is an attempt to identify the physical processes responsible for the intense winter cooling, i.e. February 2008 over AS (5–30°N and 40–80°E). The reason behind selecting 2008 is that February 2008 had the coldest winter in the last 11 years (1998–2008) from TMI (tropical rainfall measuring mission (TRMM) microwave imager) observations (Figure 1) and it is also higher than summer cooling of AS in the last 11 years. It is further confirmed with Reynolds and HadISST and concluded that such a cooling occurred only twice (1984 and 2008) in the last 30 years.

e-mail: anant@tropmet.res.in

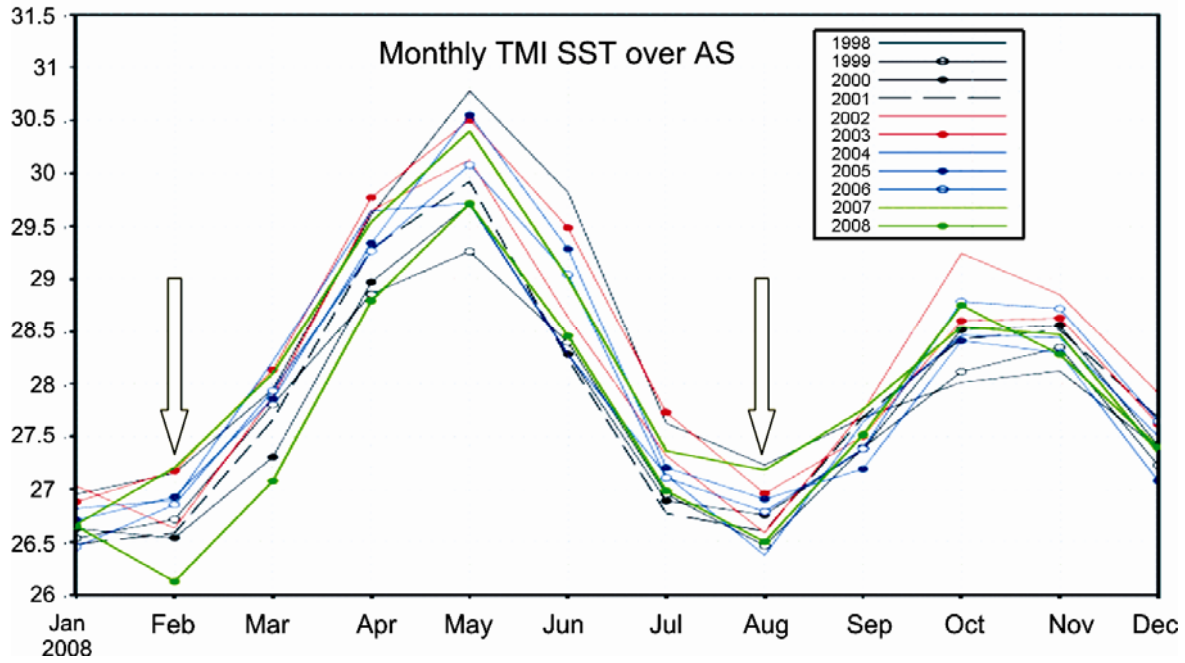

Figure 1. Time series of sea surface temperature over the Arabian Sea for the period 1998–2008 from TMI version 4.

Monthly product of the TMI SST version 4 is used for the study. The entire TMI ocean data set has been completely reprocessed and updated from version-3 to version-4 during September 2006. Monthly data for the period 1998–2007 are used for climatology preparation. TMI SST data product is reported by many authors as one of the unprecedented SST data products for regions very often having cloud cover[12,13]. The accuracy of the TMI retrieved SST with concurrent buoy observations over the north Indian Ocean is 0.65 K (ref. 14). Mean sea surface height anomaly (SSHA) data from multiple altimeter provided by AVISO as a merged product of SSHA is used for this study. TOPEX/Posedon, Jaison-1, ERS-1, ERS-2, Envisat and Geosat Altimeter observations are incorporated in the AVISOs merged product. A detailed description of this merged SSHA data is given at http://www.aviso.oceanobs.com. The operational data sets produced routinely by the Global Ocean Data Assimilation System (GODAS) developed at the National Centres for Environmental Prediction (NCEP) are utilized for the subsurface processes study. GODAS provides four-dimensional ocean states since 1980 at monthly and pentad time scales. Details of this ocean data system are given at the http://www.cpc.noaa.gov/products/GODAS/background.shtml website and by Huang *et al.*[15]. Montégut *et al.*[16] criterion is applied on GODAS temperature profile to compute mixed layer depth (MLD). The criterion is a threshold value of temperature from a near-surface value at 5 m depth (DT = 0.2°C). NCEP/National Centre for Atmospheric Research (NCAR) surface fluxes are used to compute net-surface heat flux[17] and surface vector winds from the Quikscat are utilized for the wind stress derivation. Accuracy of Quikscat retrieved wind speed and direction with concurrent observations of buoy over the north Indian Ocean is 1.57 m/s and 44.1° respectively[18]. The chlorophyll *a* data of 9 km spatial resolution from MODIS Aqua monthly products are used. This data product is generated with data processing methods similar to those applied to SeaWiFS. A description of this data set is given at http://reason.gsfc.nasa.gov/OPS/Giovanni/ocean.aqua.2.shtml. Advective heat flux computation is carried out following Shenoi *et al.*[19].

Figure 2 *a* shows SST anomaly from the TMI observation over AS for February 2008. This figure reveals anomalous cooling over AS during February 2008 (except south of 10°N and east of 70°E). Cooling higher than 1°C is found at north and northwestern AS. Similar negative anomaly over AS is also found in GODAS SST (Figure 2 *b*). This anomaly is based on more than 25 years of SST information (1980 onwards). The study was extended with Reynolds and HaDISST to establish the robustness of the cooling. These data sets also support the view that such cooling is not usual (in the last 30 years it is the second largest cooling and the areal extent of the cooling is also unusual). Studies carried out for the period 1998–2007 show that 2002, 2001, 2000 and 1999 have shown negative anomalies whereas the rest follow the positive anomaly. It is found that all the negative SST anomaly years experienced below-normal monsoon over India, 2008 (by 2%) and 2002 (by 21%) are the two

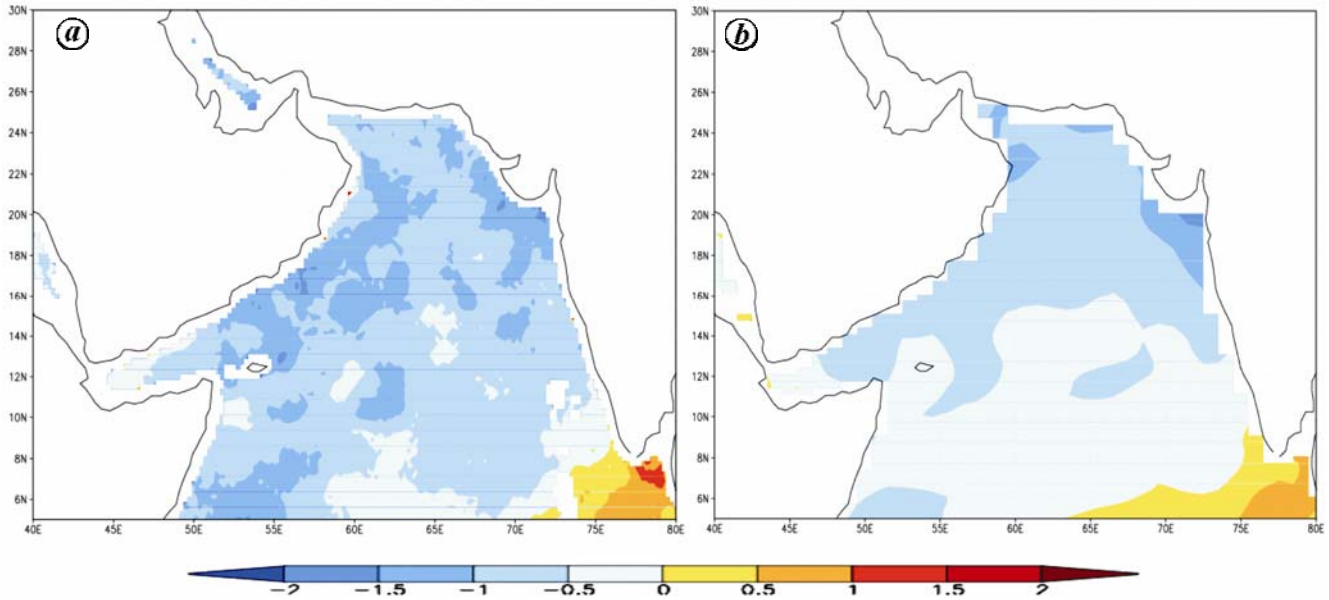

Figure 2. Sea surface temperature anomaly over the Arabian Sea from (***a***) TMI and (***b***) GODAS for February 2008.

extremes of below-normal monsoon year in the last 11 years. Information about the summer monsoon rainfall over India is taken from the website (http://www.tropmet.res.in/~kolli/MOL/Contact/frameindex.html). This supports the view that SST anomaly during pre-monsoon plays a role in the interannual variation of the monsoon[11]. Figure 3 *a* shows anomalous north westerly winds with magnitude of 4–6 m/s over the northwestern AS. This wind brings dry air from Saudi Arabia and Oman. During February 2008, relative humidity over Oman was 30% and over the western AS 70%. Air temperature over the land was higher by 6–8°C with respect to air temperature over the ocean. This may support north westerly winds anomaly over the region. Over the central and western AS (except off Gujarat and Maharasthra) winds were northerly or north westerly with a magnitude of 1.5–4 m/s. Figure 3 *b* shows the SSHA for February 2008, over the western AS, it is negative and varies between –5 and –20 cm. This corroborates the cooling condition existing over AS. Figure 3 *c* shows the chlorophyll *a* concentration over AS for February 2008. High magnitudes of chlorophyll are reported in the western AS; areal extent of the biological activity during 2008 is larger than that covered during 2003–2007. This further supports the hypothesis that decrease of ocean temperature during winter monsoon is known to enhance biological activity[7–9,20,21].

Figure 4 shows the components of surface heat flux from NCEP, Figure 4 *a* shows net-surface short-wave radiation (NSSW), Figure 4 *b* shows net-surface long-wave radiation (NSLW), Figure 4 *c* represents the latent heat flux (LH) and Figure 4 *d* shows the net-surface heat flux (Q_{netsur}) over the AS for February 2008. Relative change in sensible heat flux (SH) is small (figure not shown). Q_{netsur} is defined as

$$Q_{netsur} = NSSW - NSLW - LH - SH. \quad (1)$$

NSSW and NSLW are little deviated (10–20 W/m^2) from long-term mean over the region for February 2008. But the exchange of LH from the ocean to atmosphere is very high. Figure 4 *c* shows that latent heat loss is 180–240 W/m^2 over the western and central AS and 90–150 W/m^2 over the southeastern AS. Resultant effect of this is clearly seen in Figure 4 *d*. Q_{netsur} over AS is negative (–90 to –150 W/m^2) over western and central AS. Thus the ocean surface is losing heat flux to the atmosphere, which leads to cooling of the ocean. Southeastern AS shows positive net heat flux anomaly with magnitude around 30–60 W/m^2. Figure 5 *a* shows the mixed layer depth (MLD) over the region. Area average MLD over the AS basin is 68 m during February 2008, for the computation of the heat budget component over the basin, area averaged MLD is 75 m considered (i.e. level 7 of GODAS profile data). MLD climatology over AS[16] shows very shallow MLD over the western AS, while during February 2008 it is around 80–120 m. Resultant anomaly of the MLD is shown in Figure 5 *b*. MLD anomaly of about 30–60 m over the western AS is reported. This could be due to strong wind anomaly, which produces forced mixing and convective mixing because of cooling. Penetration of short-wave radiation below the mixed layer is computed following Paulson and Simpson[21], and Jerlov[22]. It is accounted that the short-wave radiation penetration below the mixed layer is very small in magnitude.

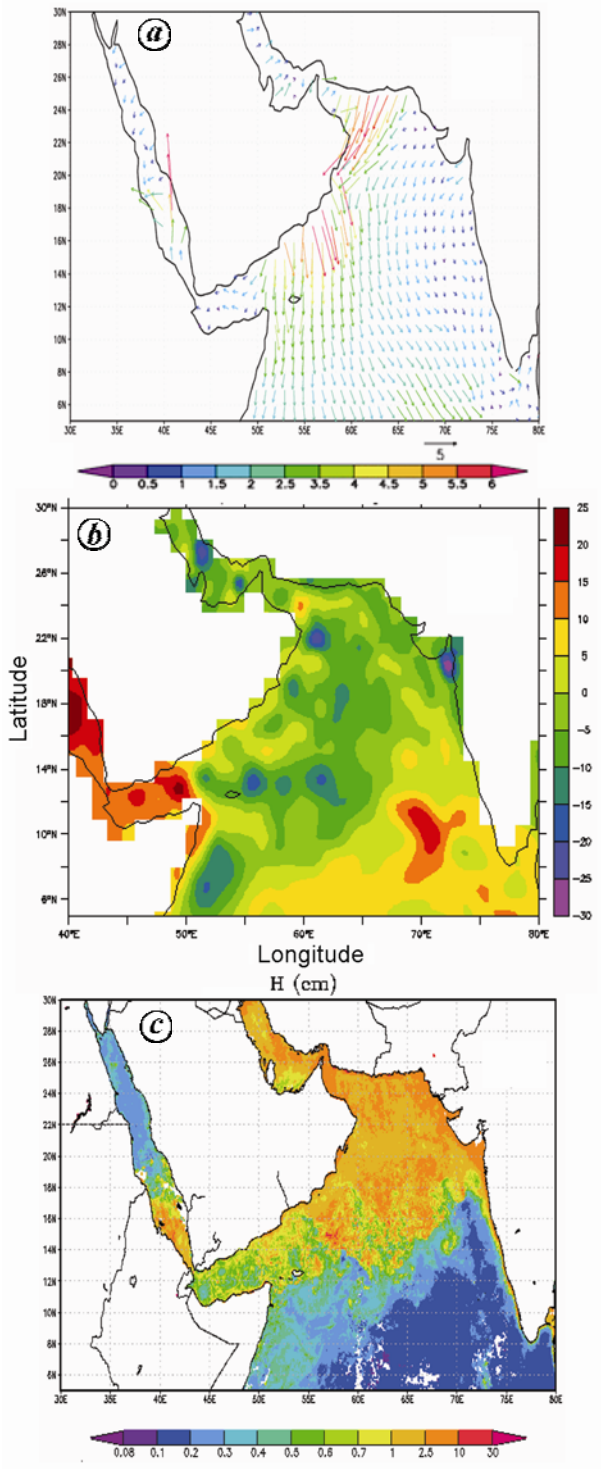

Figure 3. ***a***, Wind anomaly; ***b***, SSHA; ***c***, chlorophyll *a* concentration (mg/m^3) over the Arabian Sea for February 2008.

Turbulent diffusion flux or the vertical mixing at the base of the mixed layer with eddy diffusivity κ is given by

$$Q_{\mathrm{M}}(h) = \left[\rho_{\mathrm{s}} C_{\mathrm{p}} \kappa \left(\frac{\partial T}{\partial z}\right)\right], \tag{2}$$

where $\kappa = 1 \times 10^{-4}$ m^2/s, $\mathrm{d}T/\mathrm{d}z = 0.0089$°C/m computed using GODAS temperature profiles. C_{p} is the specific heat of water (3902 J/K/kg). The choice of κ has been guided by Zhang and Talley[23], who estimated that diathermal diffusivity at 70 m depth in the Indian Ocean varied from $< 1 \times 10^{-4}$ m^2/s at the north of 10°N and 1.3×10^{-4} m^2/s at the southern boundary (5°N). Diffusion always results in a loss of heat from the control volume. The heat loss via diffusion during February 2008 over AS is small.

The transport across the southern boundary is balanced by a mass flux through the bottom of the control volume. The difference between the vertical average of temperature at the southern boundary and the basin-wide average temperature at the bottom of the control volume results in a net flux of heat owing to this process; this heat flux is estimated as

$$Q_{\mathrm{mo}} = \rho_{\mathrm{w}} C_{\mathrm{p}} \frac{1}{A} \int \nu \, \Delta T_{\mathrm{mo}} \, \mathrm{d}x, \tag{3}$$

where ν is the transport (per unit distance along the southern boundary) through the southern boundary, and the integral is evaluated along the southern boundary.

$$\Delta T_{\mathrm{mo}} = T_{\mathrm{sb}} - \langle T \rangle = 27.75 - 25.55 = 2.20\text{°C}, \tag{4}$$

where T_{sb} is the vertically averaged temperature (over the depth of the control volume) at the southern boundary and $\langle T \rangle$ the basin-wide average of the temperature at the bottom of the control volume. These calculations are carried out using GODAS temperature profiles. Both Ekman and geostrophic flow contribute to ν; i.e. $Q_{\mathrm{mo}} = Q_{\mathrm{moe}} + Q_{\mathrm{mog}}$ and $\nu = \nu_{\mathrm{e}} + \nu_{\mathrm{g}}$.

$$\nu_{\mathrm{e}} = \frac{\tau^x}{\rho_{\mathrm{w}} f} = 4 \text{ m}^2/\text{s}. \tag{5}$$

$$\nu_{\mathrm{g}} = \frac{gD}{f} \frac{\partial n}{\partial x} = 1.55 \text{ m}^2/\text{s}. \tag{6}$$

The subscripts e and g refer to Ekman flow (geostrophic flow). The geostrophic current is assumed to be constant over the depth of the control volume. τ^x is the zonal wind stress from Quikscat observations, n the sea level from AVISO merged product, f the Coriolis parameter, $g = 9.81$ ms^{-2} the acceleration due to gravity, and D the depth of the control volume (i.e. 75 m). Horizontal gradient of sea level is computed using merged altimeter observations available from AVISO. As a result, meriodional heat flux due to the geostrophic flow is about (Q_{mog}) 12.5 W/m^2 and flux due to Ekman flow at the southern boundary is about (Q_{moe}) 33 W/m^2 for February 2008. Flux due to geostrophic flow is found to be consistent with Shenoi *et al.*[19] using long-term mean data. Flux

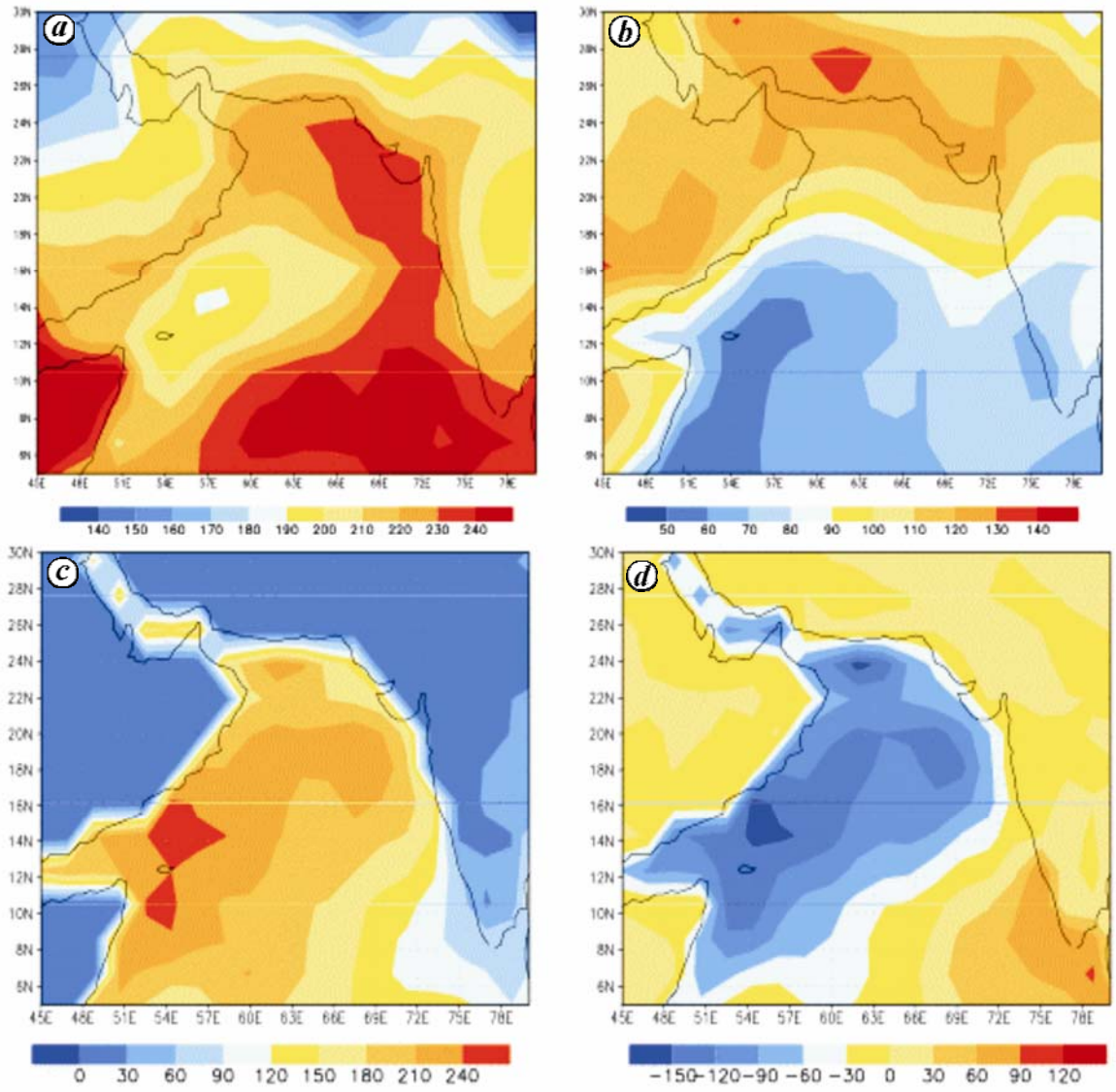

Figure 4. (***a***) Net surface short wave radiation, (***b***) net surface long wave radiation, (***c***) net latent heat flux, and (***d***) resultant net heat flux Q_{netsur} at the surface over the Arabian Sea for February 2008.

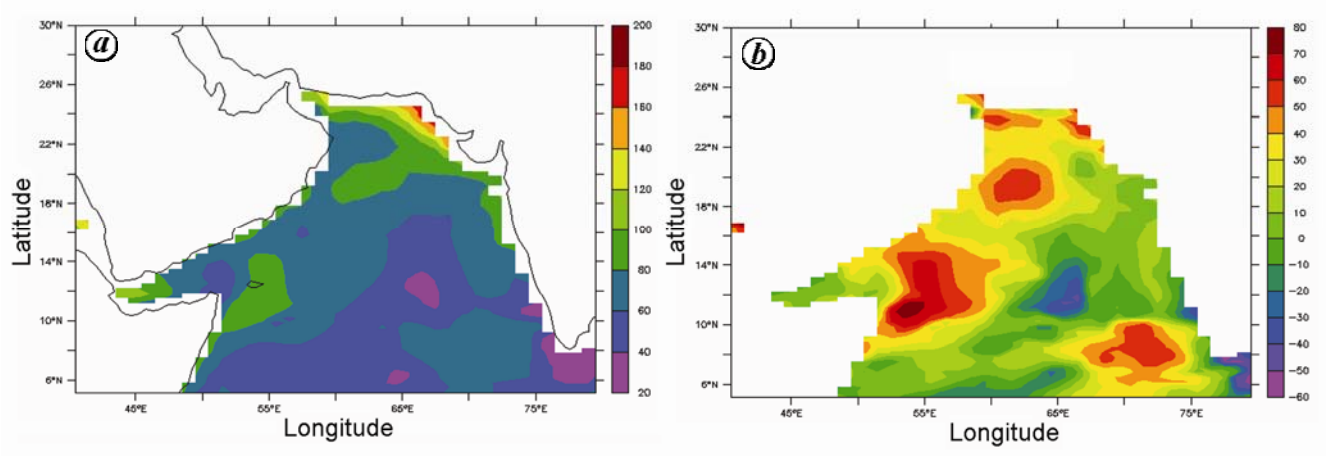

Figure 5. (***a***) Mixed layer depth and (***b***) MLD anomaly over the Arabian Sea for February 2008.

due to Ekman flow is slightly higher than that reported by Shenoi *et al.*[19]. This may be due to positive anomaly of surface wind, which influence the zonal wind stress. Thus during February 2008, AS received heat flux from the southern ocean. Resultant heat flux to AS is about –65 to –95 W/m^2 (except southeastern AS), negative sign indicates ocean is losing heat to the atmosphere. Thus major contributor towards cooling is an LH[25]. Advective processes slightly inhibit the cooling via heat flux from the southern boundary. Coastal processes are neglected in the heat budget computation.

Air-temperature gradient over Oman and western AS supports the anomalous north westerly wind. These anomalous winds bring dry air from the continent to the ocean and enhance the latent heat exchange from oceans to atmosphere. Such anomalous wind modified latent heat loss produces ocean surface cooling; cooling initiated convective mixing brings up nutrient and boosts biological activity. Biological activity increases the scope for fisheries. Anomalous winds and convective mixing deepen the mixed layer. Meridional overturning reveals that the flux due to Ekman flow and geostrophic flows are positive during winter. Anomalous winds also enhance Ekman flow at the southern boundary (it is higher than climatic mean due to anomalous zonal wind) and suppress marginally the cooling produced by LH loss. The resultant net heat flux is negative and supports the cooling over AS. This LH loss due to anomalous winds from Oman and Arabia can modify biological productivity over AS and summer monsoon rainfall over India via SST feedback.

1. Vinaychandran, P. N. and Shetye, S. R., The warm pool in the Indian Ocean. *Proc. Indian Acad. Sci.* (*Earth Planet. Sci.*), 1991, **100**, 165–175.
2. Lakshmi, V., Parekh, A. and Sarkar, A., Bimodal variation of SST and related physical processes over the North Indian Ocean: special emphasis on satellite observations. *Int. J. Remote Sensing*, 2009, **30**, 5865–5876.
3. Colborn, J., *The Thermal Structure of the Indian Ocean*, The University Press of Hawaii, 1976, p. 173.
4. Gadgil, S., Joseph, P. V. and Joshi, N. V., Ocean–atmosphere coupling over monsoon regions. *Nature*, 1984, **312**, 141–143.
5. Graham, N. E. and Barnett, T. P., Observations of sea-surface temperature and convection over tropical oceans. *Science*, 1987, **238**, 657–659.
6. Shukla, J., Effect of Arabian Sea surface temperature anomaly on Indian Summer monsoon: a numerical experiment with GFDL model. *J. Atmos. Sci.*, 1975, **32**, 503–511.
7. Madhupratap, M., Prasanna Kumar, S., Bhattathiri, P. M. A., Dileep Kumar, M., Raghukumar, S., Nair, K. K. C. and Ramaiah, N., Mechanism of the biological response to winter cooling in the northeastern Arabian Sea. *Nature*, 1996, **384**, 549–552.
8. Smith, S. L., Codispoti, L. A., Morrison, J. M. and Barber, R. T., The 1994–1996 Arabian Sea expedition: an integrated, interdisciplinary investigation of the response of the northwestern Indian Ocean to monsoonal forcing. *Deep-Sea Res. II*, 1998, **45**, 1905–1915.
9. Goes, J. I., Thoppil, P. G., Gomes, H. R. and Fasullo, J. T., Warming of the Eurasian landmass is making the Arabian Sea more productive. *Science*, 2005, **308**, 545–547.
10. Houghton, D. D., Kutzbach, J. E., McClintock, M. and Suchman, D., Response of a general circulation model to sea temperature perturbation. *J. Atmos. Sci*., 1974, **31**, 857–868.
11. Li, T., Zhang, Y., Chang, C. P. and Wang, B., On the relationship between Indian Ocean sea surface temperature and Asian summer monsoon. *Geophys. Res. Lett*., 2001, **28**, 2843–2846.
12. Harrison, D. E. and Vecchi, G. A., January 1999 Indian Ocean cooling event. *Geophys. Res. Lett.*, 2001, **28**, 3717–3720.
13. Sengupta, D., Goswami, B. N. and Senan, R., Coherent intraseasonal oscillations of ocean and atmosphere during the Asian summer monsoon. *Geophys. Res. Lett*., 2001, **28**, 4127–4130.
14. Parekh, A., Sharma, R. and Sarkar, A., A comparative assessment of surface wind speed and sea surface temperature over the Indian Ocean by TMI, MSMR and ERA-40. *J. Atmos. Ocean Technol.*, 2007, **24**, 1131–1142.
15. Huang, B., Xue, Y. and Behringer, D. W., Impacts of Argo salinity in NCEP Global Ocean Data Assimilation System: the tropical Indian Ocean, *J. Geophys. Res.*, 2008, **113**, C08002.
16. de Boyer Montégut, C., Madec, G., Fischer, A. S., Lazar, L. and Iudicone, D., Mixed layer depth over the global ocean: an examination of profile data and a profile-based climatology. *J. Geophys. Res*., 2004, **109**, C12003.
17. Kalnay, E. *et al*., The NCEP/NCAR 40-year reanalysis project. *Bull. Am. Meteorol. Soc.*, 1996, **77**, 437–471.
18. Satheesan, K. A., Sarkar, Parekh, A., Rameshkumar, M. R. and Kuroda, Y., Comparison of wind data from QuikSCAT and buoys in the Indian Ocean. *Int. J. Remote Sensing*, 2007, **28**, 2375–2382.
19. Shenoi, S. S. C., Shankar, D. and Shetye, S. R., Differences in heat budgets of the near-surface Arabian Sea and Bay of Bengal: implications for the summer monsoon. *J. Geophys. Res*., 2002, **107**, 10.1029/2000JC000679.
20. Prasanna Kumar, S. *et al*., Physical forcing of biological productivity in the northern Arabian Sea during the northeast monsoons. *Deep-Sea Res. II*, 2001, **48**, 1115–1126.
21. Paulson, C. A. and Simpson, J. J., Irradiance measurements in the upper ocean. *J. Phys. Oceanogr.*, 1977, **7**, 952–956.
22. Jerlove, N. G., *Optical Oceanography*, Elsevier, 1968, p. 194.
23. Zhang, H. M. and Talley, L. D., Heat and buoyancy budgets and mixing rates in the upper thermocline of the Indian Ocean and global oceans. *J. Phys. Oceanogr*., 1998, **28**, 1961–1978.
24. Prasanna Kumar, S. and Prasad, T. G., Winter cooling in the northern Arabian Sea. *Curr. Sci.*, 1996, **71**, 834–841.
25. Shetye, S. R., A model study of the seasonal cycle of the Arabian Sea surface temperature. *J. Mar. Res*., 1986, **44**, 521–542.

ACKNOWLEDGEMENTS. The support of Director, IITM is sincerely acknowledged. Figures are drawn using Ferret and GRADS. I thank the Remote Sensing Systems, USA for providing TMI and QuikScat data on their website. I also thank AVISO for providing merged altimeter data product and NCEP for the reanalysis data as well for the GODAS ocean data product. The chlorophyll *a* image used in this study is acquired using the Giovanni as part of the NASA's GES DISC. I am thankful to anonymous reviewers for critical comments.

Received 8 October 2009; revised accepted 12 May 2010